

Biogenic Synthesis of Gold Nanoparticles using Bark Extract of *Bauhinia variegata*: Antibacterial and *in vitro* Anticancer study

Vaghela Hiral¹, Parmar Kokila¹ and Mahyavanshi Jyotindra^{2*}

1. Department of Chemistry, Hemchandracharya North Gujarat University, Patan, 384265, Gujarat, INDIA

2. Department of Chemistry, RR Mehta College of Science and CL Parikh College of Commerce, Palanpur, 385001, Gujarat, INDIA

*mjyotindra44@gmail.com

Abstract

Our study revealed the biological synthesis of gold nanoparticles (AuNPs) using aqueous bark extract of plant named *Bauhinia variegata* (Kaachnar). Biomolecules present in the plants act as a reducing and capping agent. In this reduction reaction, gold (III) metal was reduced by biomolecules present in plants leading to formation of AuNPs. Biosynthesized AuNPs were characterized by spectral analysis (XRD, FTIR, UV-visible) and imaging microscopy. Antibacterial study of the biosynthesized AuNPs was examined against Gram-positive (*Bacillus subtilis*) and Gram-negative (*Escherichia coli*) bacteria using agar well diffusion method and AuNPs exhibited an excellent inhibition zone against mentioned bacteria. *In vitro* anticancer study of AuNPs was performed on MCF-7 cell line. Compared to standard drug, AuNPs exhibited potent anticancer activity with the IC₅₀ value 15.55 µg/ml.

Keywords: *In vitro* anticancer activity, antibacterial activity, *Bauhinia variegata*, reducing agent, nanoparticles.

Introduction

The modern approach towards nanotechnology holds nanomaterials with ability of controlling chemical and physical characteristic of the materials and to develop new nanoscale materials. Due to high surface to volume ratio and very small size, metal nanoparticles strongly received an attention in research area. Due to their extra-ordinary applications, nanoparticles are broadly investigated in various fields such as biomedical, optical devices, optics, space industries, food industries, drug delivery, cosmetics, coating, imaging, gene delivery, health care etc.¹⁶

Nanoparticles play an intermediary character among molecular or atomic structure and bulk materials. Among the noble metals (silver, platinum and palladium), gold metal nanoparticles have immense capability in applications like electron microscopy markers², DNA sequencing⁴, catalysis¹⁴ and clinical level. Various shapes of gold nanoparticles have been reported such as nanowires and nanosheets¹¹, nanotriangles²³, nanopyramids¹⁵, nanotriangles²³. Since ancient time, gold metal is used from traditional medicine to culinary items in kitchen with highly disinfectant effect. A number of scientists have reported antibacterial study using noble metal NPs¹. In recent times,

plant extract is utilized for the formation of metal nanoparticles due to easy availability, easy to handle, eco-friendly and an alternative method to other conventional methods (physical and chemical). AuNPs were effectively synthesized using micro-organism like bacteria and fungi which play a significant role in reduction reaction. Besides this, parts of plants (leaves, bark, flowers, stem cells etc.) or whole plant has also been investigated due to its effective biological applications. AuNPs with surface plasmon resonance have the ability to bind with biomolecules present in the plant such as amines and thiol group which are responsible for the reduction of HAuCl₄ to AuNPs.

Several medicinal plants have been reported in the invented story for to synthesize bio- genic AuNPs such as *Nerium oleander*²⁷, *Plumeria alba*¹⁷, *Costus pictus*²¹, *Salvia officinalis*, *Steva rebaudiana*¹³, *Acer saccharum*²⁹, *Eucomia ulmoides*⁷. In developed countries, cancer is third most leading disease cause of death after heart disease and stroke and secondary leading cause of death in the USA according to <http://www.csc.gov>. Breast cancer is the mainly leading cause death in women worldwide.

The available cytotoxic drugs used to treat breast cancer are highly expensive and not enough because due to their toxic effect in normal cells (noncancerous), they activate brutal side effects^{10,30}. That is why, the biocompatible and cost-effective novel drug should be developed. AuNPs have been used for the anticancer activity against a number of human cancer cell lines. AuNPs have attracted the research field, specifically cancer. For the diagnosis and therapy of the cancer, nanoscale drug materials effectively implicated in the body and it is found to be the new interdisciplinary research area for the researchers. AuNPs themselves inhibit the growth of blood vessels which are responsible for the growth of tumor¹⁹. AuNPs deserves an imperative stage due to drug delivery and imaging applications. AuNPs can act as specialized microscopic probes to study cancer cells, showing bright light scattering when it compiles on the surface of cancer cells. AuNPs can combine with an anticancer agent and a protein directing the behavior of surface receptors of cancer cells. Biocompatible AuNPs show toxicity according to concentration evidenced by *in vivo* and *in vitro* study. The method named γ -irradiation was used as the most excellent method at the start for the synthesis of AuNPs with high transparency and controlled size.

In contrast, microwave irradiation method has been utilized

for the preparation of AuNPs using reducing agents like cetyltrimethyl ammonium bromide (CTAB) and citric acid²⁴. Other reducing agents are also used to synthesize AuNPs such as thiophene⁸, sodium citrate²², sodium borohydride¹² and glutathione²⁵ but these are very costly and toxic.

Natural plant *Bauhinia variegata* (family *Fabaceae*) has attracted us for the biological synthesis due to its extraordinary medicinal properties of bark. The main object of the mentioned experiment was to study *in vitro* anticancer activity of biosynthesized AuNPs using bark of *Bauhinia variegata* on human breast cancer cell line (MCF- 7). Also, antibacterial activity was examined against Gram- positive (*Bacillus subtilis* MTCC 121) and Gram-negative (*Escherichia coli* MTCC 119) pathogenic bacteria. Biogenic AuNPs were characterized using spectral and imaging microscopic analysis.

Material and Methods

Material: Salt of HAuCl_4 was received from Sigma Aldrich. Healthy bark of the plant *Bauhinia variegata* was collected from the area around Patan(Gujarat). Bacterial culture was purchased from MTCC Chandigarh. MCF-7 cell culture was derived from National Centre for Cell Science (NCCS), Pune.

Preparation of plant extract: Fresh bark of the plant *Bauhinia variegata* was sterilized several times with double distilled water. Sterilized bark sample was kept for drying to remove water content at room temperature and then cut into very fine pieces. Take 10 gm of plant material (fine pieces) and boil at 70°C with double distilled 100ml water for 35 min and cool. Then the extract was filtered by using Whatmann filter paper no. 1 and stored at 4°C for further use for the synthesis.

Biogenic synthesis of gold nanoparticles: 30 ml of 1 mM HAuCl_4 solution was added to the 20 ml of bark extract, stir for 35min on magnetic hot plate at 70°C. At the initial stage of the reaction, we observed the color change from brownish to dark purple (after 1 hour) (Figure 1). Color change revealed the preliminary confirmation of formation of the gold nanoparticles. Reduction of Au^{+3} to Au^0 in the reaction mixture was due to the biomolecules in plant. Final confirmation for the formation of the gold nanoparticles was studied by UV-visible spectral analysis and surface plasmon resonance was observed at 535 nm, confirming the presence of gold nanoparticles.

Centrifugation was used to isolate AuNPs from the reaction mixture. The reaction mixture was centrifuged at 5000 rpm for 15-20 min. At bottom of the centrifuge tube, nanoparticles were observed. It was purified thrice by double distilled water, then collected and dried at 70°C in oven for about 2 hour. Dry crystalline powder of AuNPs was kept in air tight bottle for the cytotoxicity and antibacterial

study and instrumental analysis (FTIR, XRD, FEG-SEM with EDS and HR-TEM).

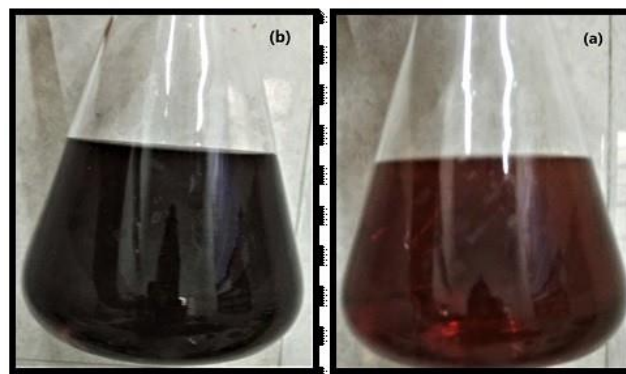


Figure 1: Color change from brownish to dark purple
 (a) bark extract of *Bauhinia variegata*
 (b) reaction mixture after completion of reaction

Characterization: Biosynthesized AuNPs were characterized using different usual modern methods. The surface plasmon resonance was recorded by UV-visible spectroscopy (Shimadzu UV 1800 UV-visible spectrophotometer). X-ray diffraction (XRD) study was carried out to pure crystalline structure with an average particle size using Rigaku D/MAX 40 kV diffractometer equipped with the graphite chromator. The average particle size was calculated by using Debye Scherer's formula:

$$D = (0.9 \lambda) / (\beta \cos \theta)$$

where D is the average crystalline size, λ is the X-ray wavelength, β is the full width at half maximum (FWHM) and θ is the diffraction angle.

Elemental composition and the structural morphology were studied by field electron gun scanning electron microscopy with energy dispersive spectroscopy (FEG-SEM with EDS) using JEOL JSM-7600F model and high resolution transmission electron spectroscopy (HR-TEM) using Tecnai G2-F30 electron microscope. Fourier transform infrared spectroscopy (FTIR) showed the functional group as biomolecules present in the plant, liable for the reduced metal ion. The antibacterial study of the biosynthesize AuNPs was examined against Gram-positive (*Bacillus subtilis* MTCC 121) and Gram-negative (*Escherichia coli* MTCC 119) pathogenic bacterial strains. The anticancer study of biogenic AuNPs was performed against human breast cancer cell line (MCF- 7).

In vitro cell viability assay (MTT assay)/(Cell Lines and Culture Medium) MCF-7 cell culture was derived from National Centre for Cell Science (NCCS), Pune. Stock cells of these cell lines were cultured in DMEM (Dulbe- coos Modified Eagles medium, low glucose with glutamine, MP biomedical), supplemented with 10% FBS (fetal bovine serum, South American origin) and also supplemented with 5 % HBSS, penicillin, streptomycin and amphotericin – B,

in a humidified atmosphere of 6 % carbon dioxide at 37°C till confluence achieved.

Screening of test compound by MTT assay (Protocol):

1. Cells were pre-incubated at an intensity of 1×10^6 cells / ml in culture medium for 3 hrs at 37°C and 6.5 % CO₂, 75 % Relative Humidity.
2. Seeding of cells was done at concentration of 5×10^4 cells / well in 100 μ l culture medium and various amounts of compound (final concentration e.g. 1000 μ g/ml – 0.05 μ g/ml) were added into microplates (tissue culture grade, 96 wells, flat bottom). Cell cultures were incubated for 24 hrs at 37°C and 6.5% CO₂.
3. 10 μ l MTT labelling mixture was added and incubated for 4 hrs at 37 °C and 6.5 % CO₂, 75 % Relative Humidity.
4. 100 μ l of solubilization solution was added in enough amount and incubated for overnight.
5. Absorbance of the samples was measured using a microplate (ELISA from Thermo, USA) reader. The wavelength to measure absorbance of the formazan product is between 540 and 600 nm according to the filters available for the ELISA reader used. (The reference wavelength should be more than 650 nm).
6. Cells with formazan product were observed at 570 nm with reference at 655 nm.
7. This experiment was performed three times for good results.

Results and Discussion

UV-visible Spectrophotometer: The aqueous reduction reaction mixture was subjected to UV-visible spectroscopy to confirm the formation of AuNPs. Reduction of Au⁺³ to Au⁰ observed by color change from brownish to dark purple is due to the excitation of surface plasmon resonance (SPR) of

AuNPs which finally confirmed the production of AuNPs. AuNPs shows absorption peak in the range of 500 to 550 nm and HAuCl₄ salt solution shows absorption peak at 312 nm. Reports showed that in aqueous solution, gold nanoparticles exhibit violet color because of an excitation of surface plasmon vibrations in the metal NPs. Here, surface plasmon resonance was observed at 535 nm (Figure 2) after completion of the reaction (dark purple color after 1 hour) which supports that biomolecules present in plant mixture extract contain strong reducing properties.

FTIR – Fourier Transform Infrared Spectroscopy: FTIR analysis was performed using Shimadzu (range 400- 4000 cm⁻¹). Biomolecules present in the plants were responsible for the reduction of the Au⁺³ ions. FTIR spectroscopy measurements were done to elucidate the biomolecules bound specifically on the surface of the gold nanoparticles and act as a reducing agent as well as capping agent. The main FTIR peak of AuNPs were observed at 3309 cm⁻¹, 3394 cm⁻¹, 2919.52 cm⁻¹, 2730 cm⁻¹, 2780 cm⁻¹, 1604.77 cm⁻¹, 1444.68 cm⁻¹ and 819 cm⁻¹ (Table 1). Vibrational stretching at 3309 cm⁻¹ and 3394.72 cm⁻¹ corresponds to O-H stretching of water and phenolic compounds.

The peaks at 2919.52 cm⁻¹, 2730 cm⁻¹ and 2780 cm⁻¹ manifest the C-H stretching for respective amines. The existence of peak at 1604.77 cm⁻¹ shows the C-C stretching in aromatic ring. The peak at 1444.68 cm⁻¹ corresponds to respective amines and the peak at 819.75 cm⁻¹ showed the presence of metal nanoparticles (AuNPs). The free NH₂ and carbonyl groups present in the proteins and amino acids residues indicate that they have capability to combine a metal. Therefore, it was concluded that the proteins could form the encapsulating layer on the metal surface (capping of gold nanoparticles) followed by stabilizing the nanoparticles.

Table 1

FTIR data of AuNPs with obtained major peaks

Functional group	Wave numbers (cm ⁻¹)
Respective amines	819 cm ⁻¹ 1444 cm ⁻¹
C-C stretching in aromatic ring	1604 cm ⁻¹
C-H stretching for respective amines	2919 cm ⁻¹ , 2730 cm ⁻¹ , 2780 cm ⁻¹
O-H stretching for water or phenolic compounds	3309 cm ⁻¹ , 3394 cm ⁻¹

Table 2

XRD pattern data of AuNPs

2 θ	Particle size (nm)	(h, k, l)	Average particle size
38.132	12.39	(111)	9.145 nm
44.284	7.49	(200)	
64.52	8.6	(220)	
77.57	8.10	(311)	

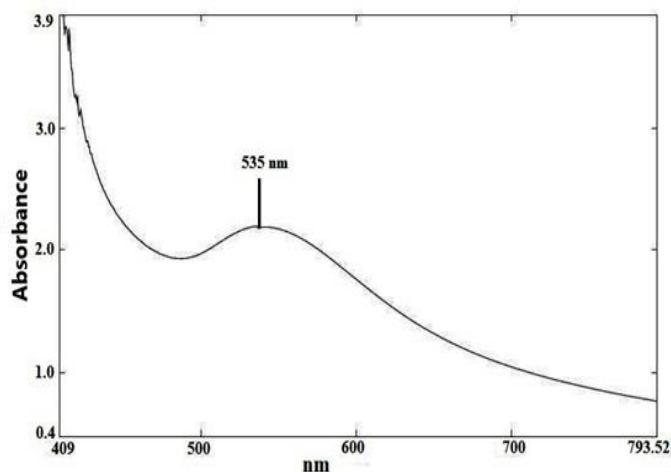


Figure 2: UV-visible spectra of biogenic AuNPs

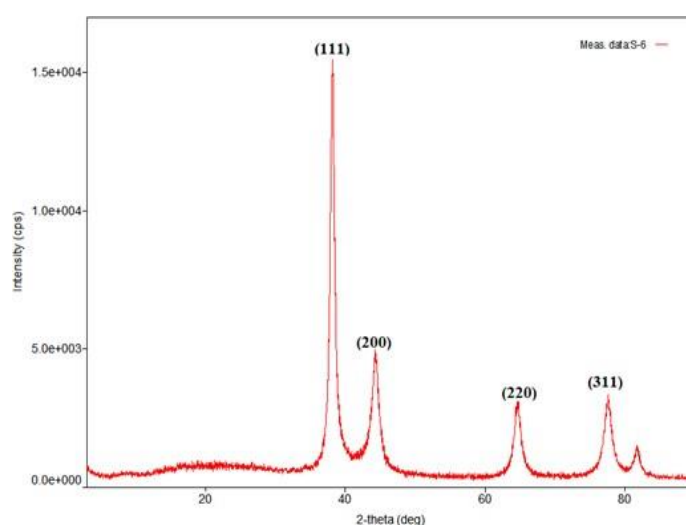


Figure 3: XRD pattern of biogenic AuNPs

XRD – X-ray Diffractometer: X-ray diffraction pattern that corresponds to the pure crystalline nature of the biosynthesized gold nanoparticles exhibits Bragg reflections which are well manifested on the basis of the face centered cubic (fcc) AuNPs. XRD pattern of the synthesized AuNPs (Figure 3) showed four diffraction peaks at 38.132, 44.284, 64.52 and 77.57 which indexed the sets of lattice planes of gold (1 1 1), (2 0 0) and (3 1 1) observed with the standard powder diffraction card of JCPDS gold file no. 01-1174. Table 2 shows the experimentally obtained X-ray diffraction angles and the standard diffraction angles of Au specimen.

The XRD study confirms that the resultant nanoparticles are FCC AuNPs. The very strong diffraction peak at 38.132 degrees is considered to be of (1 1 1) facet of the face centered cubic structure while the diffraction peaks of other gold peaks are found to be much weaker compared to standard gold nanoparticles.

Results observed are in good agreement with previous data^{Error! Reference source not found.}. An average particle size of the

CuNPs was calculated by Debye Scherrer formula:

$$D = (0.9 \lambda) / (\beta \cos \theta)$$

where D is the average crystalline size, λ is the X-ray wavelength, β is the full width at half maximum (FWHM) and θ is the diffraction angle. By calculation, the AuNPs found with 9 nm average particles size is found close to HR-TEM average particle size of ~10 nm.

FEG-SEM with EDS analysis: Field Emission Gun Scanning Electron Microscopy (FEG- SEM) analysis was performed by JEOL JSM-7600F model and showed morphological features. Analysis showed the regular spherical shape of the mono dispersed biosynthesized AuNPs with an average particle size about 2 to 10 nm (Figure 4). The elemental composition of the AuNPs was studied using energy dispersive X-ray (EDS) analysis. In figure 5, energy dispersive spectroscopy (EDS) showed the amount of gold metal with strong optical absorption peak at 1.3, 1.5, 1.7, 2.1 and 2.6 keV respectively (Table 3), showing the purity of AuNPs. The elemental amount of gold metal in mass percentage is about 56.97 % which evidenced the presence

of AuNPs.

Table 3
EDS data of AuNPs

Element	Weight %	KeV
Au	56.97	1.3, 1.5, 1.7, 2.1, 2.6

HR-TEM analysis: High Resolution Transmission Electron Microscopy (HR-TEM) was performed using Tecnai G2-

F30 model. Size and shape morphology were studied by HR-TEM. Results showed mostly spherical nature of the colloidal biosynthesized AuNPs (Figure 6). The average particle size of the AuNPs was observed around 2 to 10 nm and found to be good as compared with XRD size (9 nm) value. Using the selected area electron diffraction (SAED) pattern with bright circular spots, the crystallinity of the biosynthesized AuNPs was evidenced (Figure 6 d).

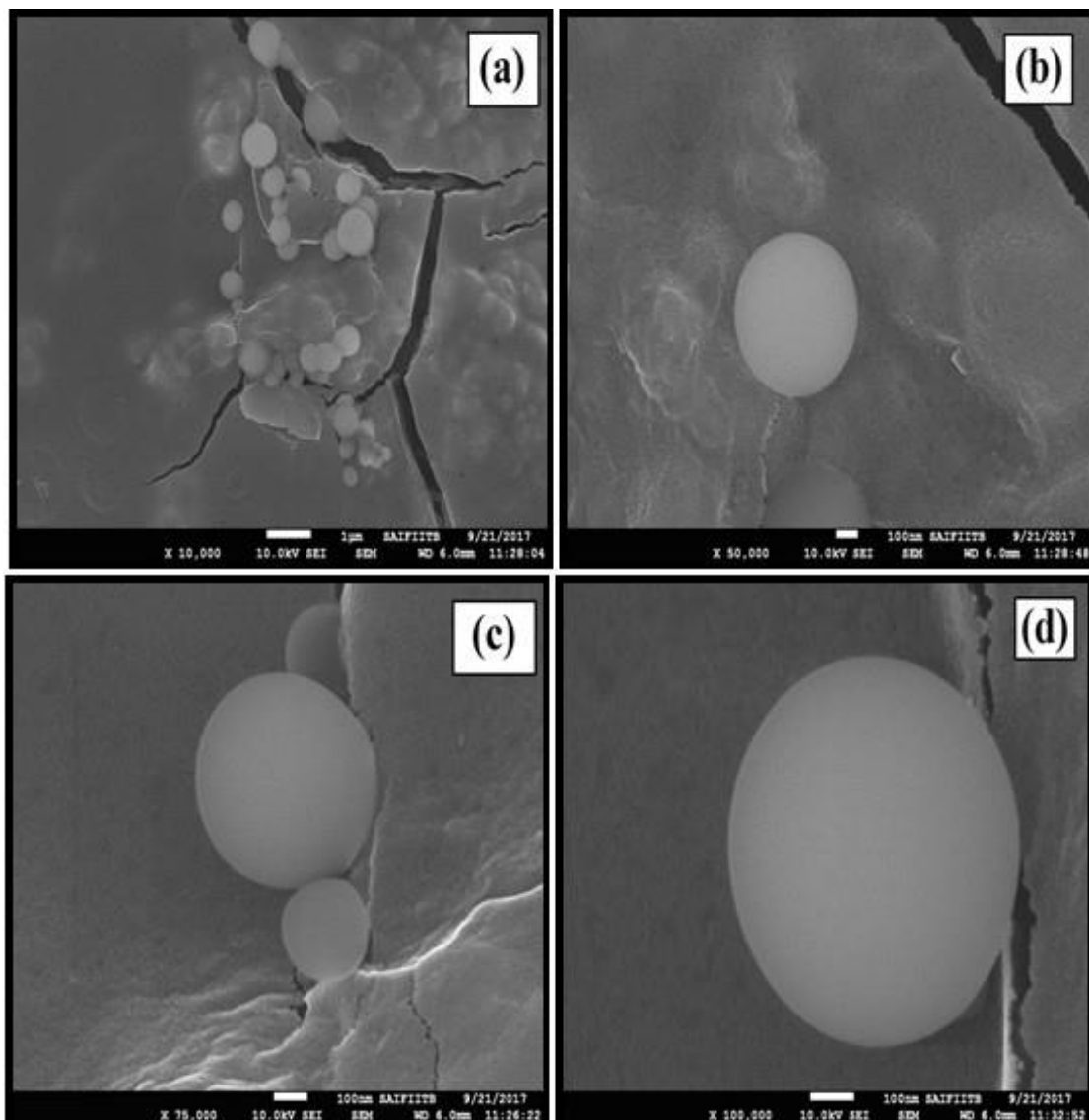


Figure 4: (a), (b), (c) and (d) are FEG-SEM images of biogenic AuNPs

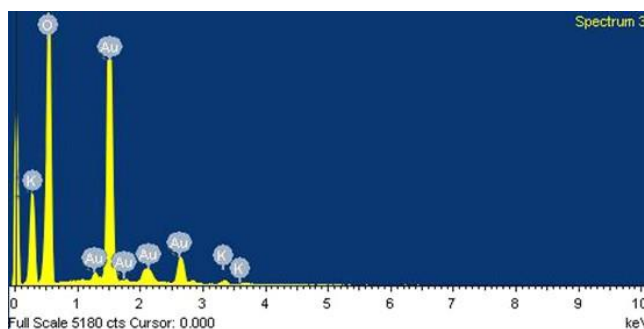


Figure 5: EDS Spattern of biologically synthesized AuNPs

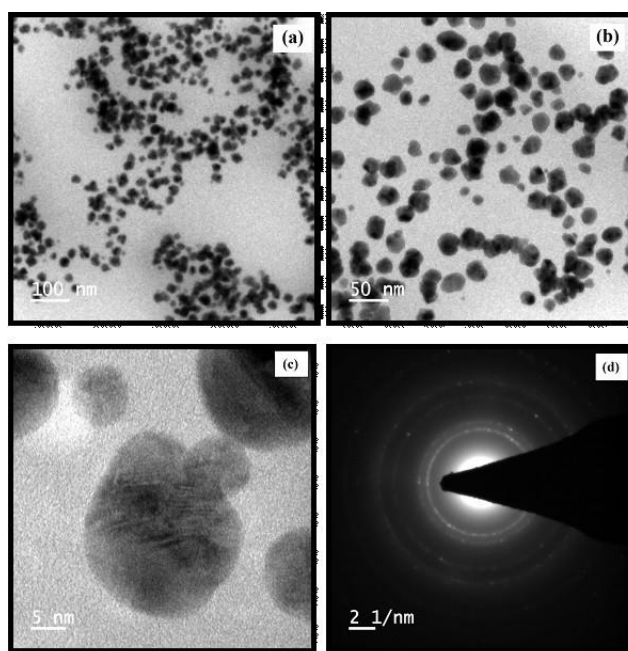


Figure 6: (a), (b) and (c) are HR-TEM of biogenic AuNPs and (d) the selected area of electron diffraction (SAED) image of AuNPs

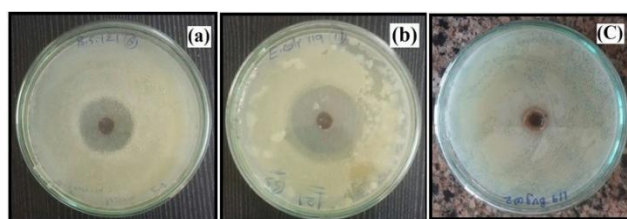


Figure 7: Antibacterial study of biosynthesized AuNPs against pathogenic bacteria (a) *Bacillus subtilis* (b) *E. coli* and (c) plant extract

Antibacterial study of Biosynthesized Gold Nanoparticles: Antibacterial activity of biosynthesized copper nanoparticles using bark extract of *Bauhinia variegata* was examined against Gram-positive (*Escherichia coli* MTCC 119) and Gram-negative (*Bacillus subtilis* MTCC 121) pathogenic bacterial strains using agar well diffusion method. Antibacterial study of plant extract was also done for the comparison. Fresh overnight culture of each bacterial strain swabbed properly by cotton on plates having sterile Muller Hinton agar and 1 well was prepared using cup borer with diameter size of 6 mm. 50 μ l of AuNPs was poured into well and disc of gentamicin was utilized as positive control. Incubate the plates for 24 hr at 37°C.

After incubation period, inhibition zone was observed around each well with the diameter in millimeter (Figure 7) (Table 4). AuNPs showed considerable zone of inhibition against both bacterial strain *Bacillus subtilis* with (10 mm) and *E. coli* (12 mm). Therefore, AuNPs synthesized from *Bauhinia variegata* can be applied as an antibacterial agent in biomedical field. Plant extract did not show any zone of inhibition. Inhibition zone of bacterial growth is due to inhibitory compound present in plant mediated AuNPs. Experiment with each strain were performed thrice for good results. However, the mechanism behind the antibacterial

activity is not clear but it was found that metal ions significantly inhibit succinate dehydrogenase, creatine kinase and many other enzymatic processes in cells⁵.

The exact mechanism of nano metals triggered antibacterial action is still being investigated, two basic phenomena has been proposed, first the toxicity arising due to the dissolution of metals from surface of nanoparticles and secondly oxidative stress via the generation of reactive oxygen species (ROS) on surface of the nanoparticles.

In vitro anticancer activity of AuNPs against MCF-7 cell lines using MTT assay: The MTT assay on MCF-7 breast cancer cell lines was performed to evaluate anticancer activity of the biosynthesized AuNPs using different doses. Nowadays, so many researchers have reported on anticancer activity of AuNPs. In our experiments, we observed that biogenic AuNPs strongly inhibit the growth of MCF-7 cancer cells more than standard drug doxorubicin. Biogenic AuNPs at different concentrations (1000 μ g/ml – 0.05 μ g/ml) exposed to MCF-7 cells for 24 hrs and % cell growth inhibition were determined using MTT assay. As a result, significant reduction in cell viability of AuNPs treated MCF-7 cells was observed at 1000 μ g/ml concentration. Cell growth inhibition of treated MCF-7 cells occurred in dose

dependent manner.

Significant cell viability of AuNPs treated cancer cells decreased by 0.24 %, 9.352 %, 17.24 %, 27.13 %, 32.65 %, 44.31 %, 54.27 %, 69.13 %, 81.27 % and 88.14 % at 0.05, 0.15, 0.46, 1.37, 4.12, 12.35, 37.04, 111.11, 333.33 and 1000 $\mu\text{g/ml}$ doses respectively. The cell specific toxicity is lost at higher doses of AuNPs and it shows maximum anticancer activity against MCF-7 cancer cells. The concentration causing 50 % cell growth inhibition (IC_{50}) was determined from DRC (Dose Response Curve) using GraphPad Prism software (Ver. 5.04) (USA). Morphological study was examined using an inverted microscope at different time intervals and compared with the cells serving as control (Figure 8(a)).

By statistical calculation, IC_{50} value of AuNPs was found to be 15.55 $\mu\text{g/ml}$ for MCF-7 cell line (Figure 8 (b)). IC_{50} value was calculated using the nonlinear regression program

origin. Plotting of graph was done against log concentration of drug on X-axis and % cell growth inhibition OR % cytotoxicity on Y-axis (Figure 9).

Conclusion

Gold nanoparticles were successfully synthesized using bark extract of *Bauhinia variegata* with aqueous HAuCl_4 salt solution. At preliminary level, formation of AuNPs was confirmed by color change from brownish to dark purple followed by UV-visible spectral analysis for final confirmation with SPR peak at 535 nm. The reduction reaction (Au^{+3} to Au^0) was very rapid and finally got completed within an hour to form AuNPs. Biomolecules responsible for the reduction of metal ions Au^{+3} were studied using FTIR analysis. Crystalline nature and face centered cubic structure with an average particle size around 9 nm of AuNPs was confirmed by XRD analysis and compared with standard JCPDS file no. 01-1174

Table 4
Antibacterial study of biosynthesized AuNPs against selective bacterial species

Bacterial Strain	Zone of Inhibition of biosynthesized Gold nanoparticles			Average zone of inhibition
	1	2	3	
<i>B. subtilis</i>	10 mm	9 mm	10 mm	10 mm
<i>E. Coli</i>	10 mm	12 mm	12 mm	12 mm

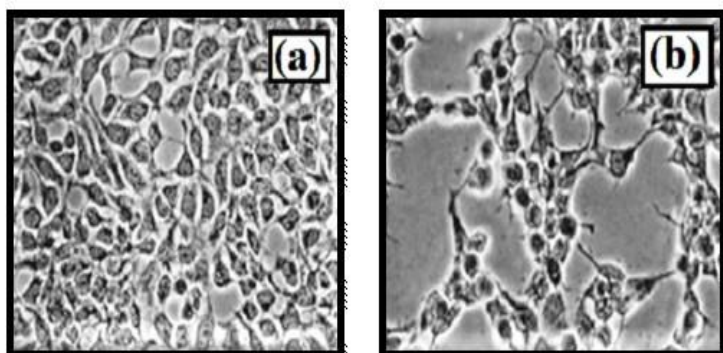


Figure 8: (a) MCF-7 control untreated cells (b) Cells treated with AuNPs

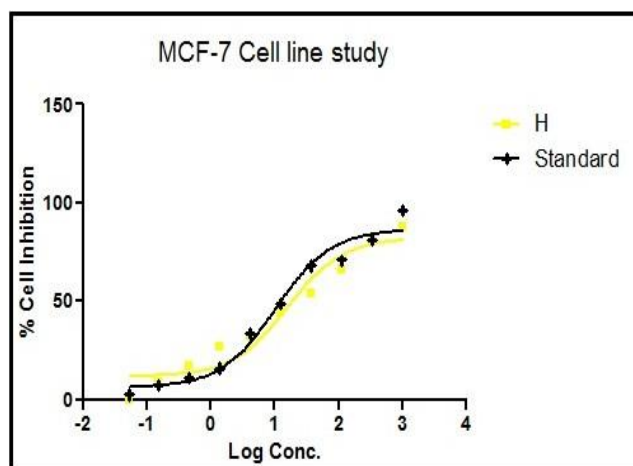


Figure 9: Dose response curve of AuNPs against MCF-7 by MTT assay

Elemental composition and morphology of the biosynthesized AuNPs were carried out using FEG-SEM with EDS and HR-TEM imaging microscopy which showed sharp regular spherical shape with particle size of 2 to 10 nm and showed considerable crystallinity and stability. Antibacterial activity of AuNPs mediated from *Bauhinia variegata* was performed against Gram +Ve (*Bacillus subtilis*) and Gram -Ve (*Escherichia coli*) and exhibited considerable zone of inhibition.

Compared to standard drug biogenic AuNPs exhibited potent anti-proliferative efficacy against MCF-7 cells with the low IC₅₀ value 15.55 µg/ml. This investigation described the eco-friendly and cost effective biological method to synthesize AuNPs for effectual antibacterial and anticancer activities. The experiments implicate that the biologically synthesized AuNPs may show the way to precious discoveries in biomedical applications.

Acknowledgement

The authors are thankful to UGC India for providing fellowship to one of the authors Ms. Hiral Vaghela. The authors are also thankful the HNGU, Patan, MTCC Chandigarh and NCCS Pune.

References

1. Bankura K., Maity D., Mollick M., Mondal D., Bhowmick B., Bain M., Chakraborty A., Sarkar J., Acharya K. and Chattopadhyay D., Evaluation of the physicochemical properties and antioxidant activity of carboxymethyl chitosan nanoparticles, *Carbohydrate Polymers*, **89**, 1159–1165 (2012)
2. Baschong W. and Wrigley N., A simple method for the visualization of proteins and lipids in transmission electron microscopy, *J. Electron Microscopy Technique*, **14**, 313–323 (1990)
3. Dash P. and Balto Y., Morphological and structural studies on ZnS nanoparticles synthesized by co-precipitation technique, *Res. J. Nanosci. Nanotechnol.*, **1**, 25–33 (2011)
4. Elghanian R., Storhoff J., Mucic R., Letsinger R. and Mirkin C., Selective colorimetric detection of polynucleotides based on the distance-dependent optical properties of gold nanoparticles, *Science*, **277**, 1078–1081 (1997)
5. Franco-Molina M., Mendoza-Gamboa E., Sierra-Rivera C., Gómez-Flores R., Zapata-Benavides P., Castillo-Tello P., Alcocer-González J., Miranda-Hernández D., Tamez-Guerra R. and Rodríguez-Padilla C., Antitumor activity of colloidal silver on MCF-7 human breast cancer cells, *J. Exp. Clin. Cancer Res.*, **29**, 148–148 (2010)
6. Gardea-Torresdey Jorge L., Gomez Eduardo, Peralta-Videa Jose R., Parsons Jason G., Troiani Horacio and Jose-Yacamán Miguel, Alfalfa sprouts: a natural source for the synthesis of silver nanoparticles, *Langmuir*, **19**, 1357–1361 (2003)
7. Guo M., Li W., Yang F. and Liu H., Synthesis and photoluminescence properties of Eu³⁺-doped Y₂O₃ nanocrystals, *Spectrochim. Acta Part A*, **142**, 73–79 (2015)
8. Guo Q., Zou S., Li J., Li D., Jiao H. and Shi J., Preparation and photocatalytic activity of TiO₂ nanoparticles modified with Au and Pt for degradation of Rhodamine B, *J. Nanoparticle Res.*, **16**, 2702–2702 (2014)
9. Jain S., Hirst D. and O'Sullivan J., Gold nanoparticles as novel agents for cancer therapy, *Br. J. Radiol.*, **85**, 101–113 (2012)
10. Kim D., Hong G., Lee H., Choi S., Chun B., Won C., Hwang I. and Won M., Microscale 3D hydrogel scaffold for biomimetic gastrointestinal (GI) tract model, *Int. J. Neurosci.*, **117**, 387–400 (2007)
11. Kim J., Cha S., Shin K., Jho J. and Lee J., A water-dispersible organic dye complex showing amplified spontaneous emission and high sensitivity to volatile organic compounds, *Adv. Mater.*, **16**, 459–464 (2004)
12. Kim J., Kim J., Chung S. and Chung B., A novel method for the synthesis of gold nanoparticles using aromatic disulfides, *Analyst*, **134**, 1291–1291 (2009)
13. Khan A., Behlol A., Subramanian S., Sivasubramanian A., Veerappan G. and Veerappan A., Synthesis and characterization of silver nanoparticles using *Caesalpinia pulcherrima* leaf extracts and their biomedical applications, *Spectrochim. Acta Part A*, **130**, 54–58 (2014)
14. Li J., Ma C., Xu X., Yu J., Hao Z. and Qiao S., Photocatalytic degradation of azo dye acid red 14 in aqueous suspensions of TiO₂: reaction kinetics and mechanism, *Environ. Sci. Technol.*, **42**, 8947–8951 (2008)
15. Lin T., Linn N., Tarajano L., Jiang B. and Jiang P., Enhanced Photocatalytic Activity of TiO₂ Films via Surface Functionalization with Ag Nanoparticles, *The Journal of Physical Chemistry C*, **113**, 1367–1372 (2009)
16. Mata R., Bhaskaran A. and Sadras S., Green Synthesis of Silver Nanoparticles Using Bark Extract of *Syzygium cumini* (L.) and Evaluation of Their Antimicrobial Activity, *Particuology*, **24**, 78–86 (2016)
17. Meguellati H., Ouafi S., Saad S., Harchaoui L. and Djemouai N., Somatic embryogenesis and evolution of phenolic compounds production in *Teucrium polium* L. subsp. *geyrii* Maire cell suspensions, *Res. J. Biotech.*, **17**(9), 1–12 (2022)
18. Mollick Md., Masud R., Bhowmick B., Mondal D., Maity D., Rana D., Dash S., Chattopadhyay S., Roy S., Sarkar J., Acharya K., Chakraborty M. and Chattopadhyay D., Eco-friendly approach towards synthesis of zinc oxide nanoparticles and their potential application as photocatalytic degradation of commercial textile dye, *RSC Adv.*, **4**, 37838–37838 (2014)
19. Mlurugan M., John K., Anthony P., Jeyaraj M., Krishnaraj N. and Gurunathan S., Biofabrication of gold nanoparticles and its biocompatibility in human breast adenocarcinoma cells (MCF-7), *J. Ind. Eng. Chem.*, **20**(4), 1713-1719 (2014)
20. Mallikarjuna K., Sushma N., John R., Subba B., Narasimha G. and Raju B., Prasad D., Green Synthesis of Silver Nanoparticles Using Leaf Extract of *Mimusops elengi* Linn. for Enhanced Antibacterial Activity, *Int. J. Chem. Anal. Sci.*, **4**, 14–18 (2013)

21. Nakkala Jayachandra, Reddy Bhagat, Ekta Suchiang, Kitlangki and Sadras Sudha Rani, Green synthesis and characterization of silver nanoparticles using *Lantana camara* leaf extract, *J. Mater. Sci. Technol.*, **31**, 986–994 (2015)
22. Qiao X., Liu X., Li X. and Xing S., Ultrasensitive detection of dopamine using a DNA aptamer-based carbon nanotube modified screen-printed electrode, *New J. Chem.*, **39**, 8588–8593 (2015)
23. Rai A., Singh A., Ahmad A. and Sastry M., Stable silver nanoparticles as colorimetric sensor for ammonia detection, *Langmuir*, **22**, 736–741 (2006)
24. Rezende T., Andrade G., Barreto L., Costa N., Gimenez I. and Almeida L., Synthesis, characterization and photocatalytic properties of ZnO powders obtained by combustion method, *Mater. Lett.*, **64**, 882–884 (2010)
25. Ramalingam B., Parandhaman T. and Das S., Biocompatible Chitosan-Poly(Vinyl Alcohol) Hybrid Nanofiber Matrices for Wound Dressing Applications, *ACS Appl. Mater. Interfaces*, **8**, 4963–4976 (2016)
26. Sabaratnam V., Gurunathan S., Raman, J., Malek S. and John P., Green synthesis and characterization of silver nanoparticles using *Ganoderma austral*, *Int. J. Nanomedicine*, **8**, 4399–4399 (2013)
27. Tahir K., Nazir S., Li B., Khan A., Khan Z., Gong P., Xia H. and Li B., Antimicrobial, cytotoxic, phytotoxic and antioxidant potential of silver nanoparticles synthesized using *Crambe abyssinica* aqueous leaf extract, *Mater. Sci. Eng. C*, **156**, 148–158 (2018)
28. Vankar P. and Shukla D., Biosynthesis of silver nanoparticles using lemon leaves extract and its application for antimicrobial finish on fabric, *Appl. Nanosci.*, **2**, 163–168 (2012)
29. Vellaian Sathish, Shanmugam Kowsalya and Subramaniam Umavathi, GC-MS analysis and Larvicidal activity of *Plectranthus amboinicus* and *Sphagneticola calendulacea* leaf extract in relation to larvicidal activity against the mosquito *Aedes aegypti*, *Res. J. Biotech.*, **18(1)**, 36–42 (2023)
30. Yang S., Zhang Z., Thomas A. and Wang X., Aerogels: Synthesis, characterization and applications, *Angew. Chem. Int. Ed.*, **8**, 1–25 (2009).

(Received 08th April 2023, accepted 15th June 2023)